Chapter 2
Synthesis of a Porphyrin-Fused π-Electron System

Hidemitsu Uno, Kazunari Tagawa, Hajime Watanabe, Naoki Kawamoto, Mina Furukawa, Tetsuo Okujima, and Shigeki Mori

Abstract Oligoporphyrins with a large fused π-electron system were successfully synthesized by the fusion of porphyrin chromophores with polycyclic aromatic hydrocarbons (PAHs). Oligoporphyrins fused with benzene units and zinc diporphyrins fused with PAHs were prepared and their electronic properties were examined. Electronic spectra showed strong absorption in the red to near-infrared (NIR) region. Not only the absorption maxima but also the number of absorption bands was affected by the fusion mode of the porphyrin chromophores. In the UV-vis spectra of the oligoporphyrins, three major absorption bands corresponding to Soret and Q bands were observed. A linearly fused trizinc triporphyrin with two benzene moieties showed strong Q-band absorption at 680 nm, while split Q-band absorptions at 663 and 674 nm were observed in the L-shaped triporphyrin. Preparation based on the retro-Diels-Alder reaction of the precursors with a bicyclo[2.2.2]octadiene skeleton did not give naphthacene- and pentacene-fused diporphyrins but instead gave naphthalene-, anthracene-, and chrysene-fused diporphyrins. In the chrysene-fused diporphyrin, the absorption maximum in the Q band was 624 nm, which was similar to that of naphthalene-fused diporphyrin.

Keywords Porphyrinoid • Benzene-fused diporphyrin • Doubly benzene-fused triporphyrin • Triply benzene-fused tetraporphyrin • Quadruply benzene-fused pentaporphyrin • Retro-Diels-Alder reaction • Bicyclo[2.2.2]octadiene • Acene-fused diporphyrin • Pericyclic reaction • Near infrared • Two-photon absorption • [3 + 1] porphyrin synthesis • Cyclo-tetramerization

H. Uno (✉) • K. Tagawa • H. Watanabe • M. Furukawa • T. Okujima
Department of Chemistry and Biology, Graduate School of Science and Engineering, Ehime University, Matsuyama 790-8577, Japan
e-mail: uno@ehime-u.ac.jp

N. Kawamoto • S. Mori
Integrated Center for Sciences, Ehime University, Matsuyama 790-8577, Japan

T. Akasaka et al. (eds.), *Chemical Science of π-Electron Systems*,
DOI 10.1007/978-4-431-55357-1_2

2.1 Introduction

NIR dyes have garnered increasing attention due to their applicability as singlet oxygen sensitizers for photodynamic therapy [1], two-photon microscopic imaging agents [2], sensitizers for TiO_2-based organic photovoltaics [3], cutoff filters [4], and so on. For the former two applications, good permeability of light in living cells is essential. As water and hemoglobin are the major light-absorbing materials in mammalian cells, there is a light-permeable region with an optical window roughly from 600 to 1300 nm [5]. The use of NIR light for organic solar cells was keenly investigated in order to improve their performance [6], as more than 40 % of the solar energy reaching to the earth's surface is from NIR light.

These compounds are rather difficult to synthesize due to their instability under oxidizing conditions caused by their intrinsically high HOMO energy levels. They are also insoluble in common solvents due to the stacking nature of their large flat chromophores. The solubility is commonly improved by introducing solubilizing substituents such as long, branched alkyls [7] or bulky groups [8], which prevent the stacking of the flat chromophores. From the point of view of a synthetic strategy, fusion by construction of aromatic rings between the chromophore units at the very end of the synthesis is more advantageous than the successive expansion of chromophores. When the porphyrin system is employed, fusion method is thought to be ideal because the system is robust and reactive. There are two methods for the construction of fusing aromatic units (Fig. 2.1). In the first method, the targeted π-systems **2** are created by the construction of the fusing aromatic system such as benzene [9], thiophene [10], *etc*. [11] between the singly connected chromophore units **1** (Fig. 2.1a). In the second method, the targeted compounds **4** bearing the benzene unit are formed from the precursors **3** by pericyclic cycloreversion [12], oxidation [13], or rearrangement (Fig. 2.1b). In these methods, the purification of the target products is still a severe problem. Nanographenes are prepared by the

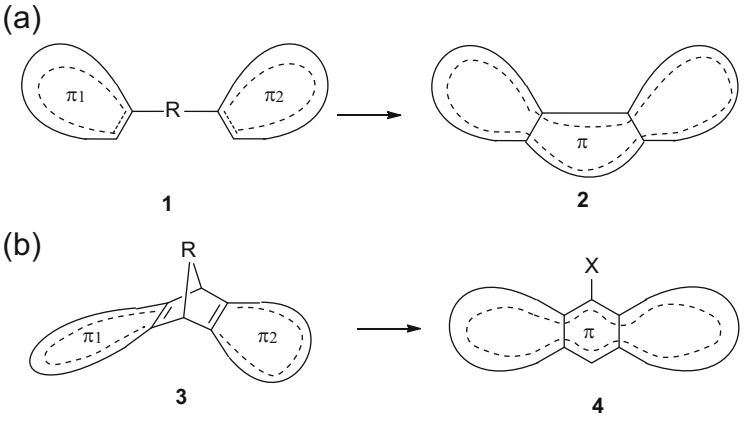

Fig. 2.1 Strategy for the construction of fusing aromatic units

former strategy from the well-designed polyphenyl derivatives based on the 6π-electrocyclic reaction, followed by thermal dehydrogenation [14]. The pericyclic cycloreversion in the latter method is one of the most advantageous reactions for the construction of such fusing π-systems, because this reaction can be conducted without reagents or solvents. Only the activation energy is required for the reaction, and no purification is needed, if the reaction occurs quantitatively. In this session, we have discussed our recent results on the preparation of large π-system based on the fusion of chromophores in the last stage of the synthesis.

2.2 Oligoporphyrins Fused with Benzene Units

Oligoporphyrins with fused π-systems are very attractive not only as NIR absorbing dyes but also as two-photon absorbing materials applicable to laser scanning fluorescence microscopy [15] and fine focused photodynamic therapy for inner tissues [16]. An important factor for large two-photon absorbing cross-section values is a coplanar geometry between neighboring porphyrin chromophores in order to maximize π-electron delocalization throughout the molecular network [17]. In order to know the effect of π-system shapes, various kinds of porphyrin oligomers fused with benzene moieties were prepared.

Bicyclo[2.2.2]octadiene (BCOD)-fused oligoporphyrins were synthesized and converted to the targeted fully fused oligoporphyrins by the retro-Diels-Alder reaction in the final step. First, the synthesis of porphyrins fused with pyrrole through the BCOD moiety (Scheme 2.1) was carried out. A pyrrole ring was constructed at the double bond of the BCOD-fused pyrrole-2-carboxylate ethyl

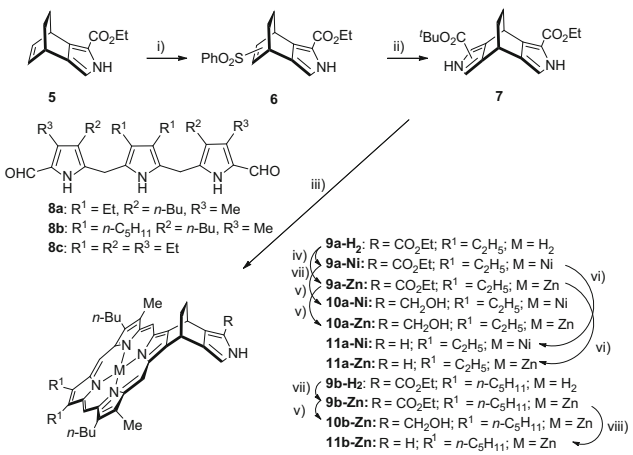

Scheme 2.1 *Reagents and conditions:* (i) PhSCl, CH_2Cl_2, −78 °C; *m*CPBA, CH_2Cl_2, 0 °C; DBU, CH_2Cl_2, rt; (ii) $CNCH_2CO_2{}^tBu$, KO^tBu, THF, −78 °C to rt; (iii) TFA, rt; **8**, CH_2Cl_2, rt; Et_3N, DDQ, rt; (iv) $Ni(OAc)_2 \cdot 4H_2O$, CH_2Cl_2, reflux; (v) $LiAlH_4$, THF, rt; (vi) NaOH, ethylene glycol; 170 °C; (vii) $Zn(OAc)_2 \cdot 2H_2O$, CH_2Cl_2, rt; (viii) NaOH, ethylene glycol; 170 °C; $Zn(OAc)_2 \cdot 2H_2O$, CH_2Cl_2, rt

ester **5** [18] by consecutive treatment with PhSCl, *m*-chloroperbenzoic acid (*m*CPBA), 1,4-diazabicyclo[5.3.0]undec-11-ene (DBU), and a potassium salt of *tert*-butyl isocyanoacetate. A regioisomeric mixture of *tert*-butyl ethyl dipyrroledicarboxylate **7** [19] was obtained with a good overall yield. The tripyrranes **8a** and **8b** were prepared according to procedures described in the literature [20] and then condensed with **7** by treatment with trifluoroacetic acid (TFA) followed by oxidation with DDQ. The pyrroloporphyrins **9a-H$_2$** and **9b-H$_2$** were each obtained with a yield of 27 %. The free-base pyrroloporphyrin **9a-H$_2$** was metalated with nickel acetate and zinc acetate to give the nickel and zinc porphyrins **9a-Ni** and **9a-Zn**, respectively, with good yields. Similarly, the zinc porphyrin **9b-Zn** was obtained with a yield of 93 %. The ester moiety of **9** was reduced with $LiAlH_4$ at 0 °C to give hydroxymethyl derivatives **10**, which were purified by short-column chromatography on silica-NH_2 gel. The ethyl ester group of **9** was removed by heating at 170 °C in an alkaline solution of ethylene glycol to give α-free pyrroloporphyrins **11** with a good yield.

2.2.1 Preparation of Benzene-Fused Diporphyrins

For the preparation of BCOD-connected diporphyrins, free-base pyrrole-connected porphyrins **11** were subject to inverse [3 + 1] porphyrin synthesis with tripyrranedicarbaldehydes **8**. Metalation with $Zn(OAc)_2 \cdot 2H_2O$ and $Cu(OAc)_2 \cdot H_2O$ gave dimetallodiporphyrins **12** with a moderate yield (12–33 %) (Scheme 2.2) [19, 21]. As the nickel porphyrin was stable under the acidic conditions employed in the [3 + 1] porphyrin synthesis [21], diporphyrins were prepared with two different metals. On the other hand, the zinc porphyrin was labile under the reaction conditions, such that only dizinc derivatives could be prepared.

The absorption and fluorescence maxima of the dimers are summarized in Table 2.1. The Soret and Q bands of the zinc-porphyrin monomer **9a-Zn** appeared at slightly longer wavelength [403 (log $\varepsilon = 5.49$), 532 (4.19), and

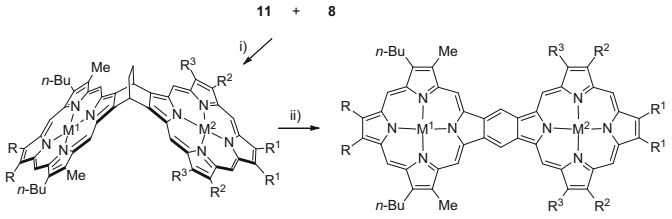

12aa-Zn$_2$: M^1 = M^2 = Zn, R = R^1 = Et, R^2 = *n*-Bu, R^3 = Me
12ac-Zn$_2$: M^1 = M^2 = Zn, R = R^1 = R^2 = R^3 = Et
12aa-NiZn: M^1 = Ni, M^2 = Zn, R = R^1 = Et, R^2 = *n*-Bu, R^3 = Me
12aa-NiCu: M^1 = Ni, M^2 = Cu, R = R^1 = Et, R^2 = *n*-Bu, R^3 = Me
12ac-NiZn: M^1 = Ni, M^2 = Zn, R = R^1 = R^2 = R^3 = Et
12bb-Zn$_2$: M^1 = M^2 = Zn, R = R^1 = *n*-C$_5$H$_{11}$, R^2 = *n*-Bu, R^3 = Me
12b-Zn$_2$: M^1 = M^2 = Zn, R = R^1 = R^2 = R^3 = *n*-C$_5$H$_{11}$

13aa-Zn$_2$
13ac-Zn$_2$
13aa-NiZn
13aa-NiCu
13ac-NiZn
13bb-Zn$_2$
13b-Zn$_2$

Scheme 2.2 *Reagents and conditions:* (i) TFA, CH_2Cl_2, rt; Et_3N; DDQ; $Zn(OAc)_2 \cdot 2H_2O$ or $Cu(OAc)_2 \cdot 2H_2O$, CH_2Cl_2, rt; (ii) 170 °C, in vacuo

Table 2.1 Absorption and emission maxima of benzene-fused oligoporphyrins

Oligoporphyrin	λ_{max} /nm (log ε)						Fluorescence/nm
	Band I		Band II		Band III		
12aa-Zn$_2$[a]	399	414			533	574	579
	(5.65)	(5.65)			(4.65)	(4.74)	624
12aa-NiZn[a]	394	410			555	572	578
	(5.42)	(5.49)			(4.53)	(5.72)	
13aa-Zn$_2$[b]	390	412	444	474	621	636	641
	(4.98)	(4.91)	(4.90)	(5.40)	(4.78)	(5.27)	
13aa-NiZn[b]	389		470	477	619	635	–
	(4.94)		(5.13)	(5.15)	(4.73)	(5.21)	
13aa-NiCu[a]	400		466		580	634	–
	1.00[c]		0.92[c]		0.22[c]	0.89[c]	
15b-Zn$_3$[b]	409	416	493		626	680	683
	(5,14)	(5,14)	(5.40)		(4.58)	(5.55)	
19b-Zn$_3$[b]	412	427	486		663	674	677
	(5.18)	(5.18)	(5.36)		(5.39)	(5.45)	
20b-Zn$_4$[b]	412	427	496		682	716	721
	(5.41)	(5.18)	(5.53)		(4.76)	(5.71)	
21b-Zn$_5$[b]	414	437	497	579	722	762	767
	(5.62)	(5.32)	(5.48)	(4.85)	(4.90)	(5.80)	

[a]In $CHCl_3$
[b]1% pyridine/ $CHCl_3$
[c]Intensity ratio

570 (4.24) nm] than those of **9a-Ni** [394 (5.28), 516 (4.04), and 554 (4.37) nm]. The bicyclo[2.2.2]octadiene-bridged dimers **12aa-NiZn** and **12 ac-NiZn** exhibit two Soret bands at 394 (5.42) and 410 (5.49) nm and three Q bands at 535 (4.40), 555 (4.53), and 572 (4.50) nm. The shorter-wavelength Soret-band absorption appeared at almost the same position as for the parent nickel porphyrin **9a-Ni** with a slightly larger intensity. In contrast, the longer-wavelength Soret band was absorbed at a lower energy field compared to that of zinc porphyrin **9a-Zn**, with almost the same intensity. Even in the case of the symmetric zinc-porphyrin dimers **12aa-Zn$_2$** and **12bb-Zn$_2$**, two separated Soret bands with the similar intensity (log $\varepsilon = 5.65$) were observed at 399 and 414 nm. This phenomenon is due to the exciton coupling between the porphyrin rings through the bicyclo[2.2.2]octadiene moiety [22].

In the UV-vis spectra of the benzene-fused diporphyrins **13**, there are three major absorption bands. The two bands (band I: 380–440 and band II: 440–580 nm) in the shorter-wavelength region correspond to Soret bands and the remaining major band (band III) is the Q band. The absorption and emission maxima in the UV-vis-NIR spectra of the dimers are summarized in Table 2.1. The longest-wavelength absorptions in the Q-band region (band III) become quite strong due to the fusion of porphyrin chromophores. In the fluorescence spectra, small Stokes' shifts (3–5 nm) are observed [23].

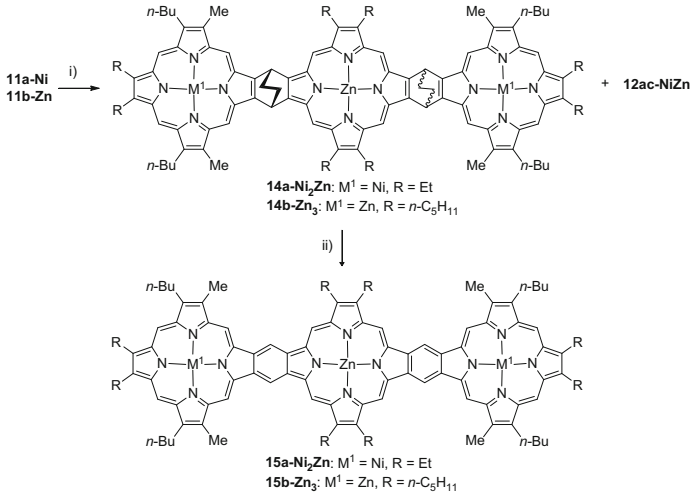

Scheme 2.3 Reagents and conditions: (i) 3,4-diethyl-2,5-bis(hydroxymethyl)pyrrole or 3,4-dipentyl-2,5-bis(hydroxymethyl)pyrrole, $BF_3 \cdot OEt_2$, CH_2Cl_2, rt; chloranil, $Zn(OAc)_2{\cdot}2H_2O$, 50 °C; (ii) 200 °C, in vacuo

2.2.2 Preparation of Benzene-Fused Tri-, Tetra-, and Pentaporphyrins

BCOD- and benzene-fused oligoporphyrins were prepared using the following method. The [2 + 2] porphyrin synthesis using α-free pyrroloporphyrins **11** and 2,5-bis(hydroxymethyl)pyrroles was first employed for the construction of linearly connected triporphyrins. An equal molar mixture of nickel porphyrin **11a-Ni** and 3,4-diethyl-1,5-bis(hydroxymethyl)pyrrole was successively treated with $BF_3 \cdot OEt_2$, chloranil, and zinc acetate to give a *syn*- and *anti*-mixture (*ca.* 1:1) of linear triporphyrin **14a-Ni$_2$Zn** at a yield of 45 % with a small amount (5 %) of diporphyrin **12 ac-NiZn** (Scheme 2.3). The *syn*- and *anti*-isomers (C_{2v} and C_{2h} point groups, respectively) of **14a-Ni$_2$Zn** were separated by fractional recrystallization after preparative GPC, and the structures were unambiguously determined by X-ray crystallography. Thermogravimetric (TG) analysis revealed that the triporphyrin **14a-Ni$_2$Zn** expelled two molecules of ethylene between 170 and 200 °C. No spectroscopic evidence of triporphyrin **15a-Ni$_2$Zn** was obtained due to its insoluble nature. In order to solubilize the linear triporphyrin, its ethyl and nickel moieties were changed to pentyl and zinc groups, respectively. Similar reactions of the nickel porphyrin **11b-Zn** and 3,4-dipentyl-1,5-bis(hydroxymethyl)pyrrole, however, did not produce the intended **14b-Zn$_3$** at all. Furthermore, the synthesis of **14a-Ni$_2$Zn** could not be reproduced. All trials, except for the first one mentioned above, produced only a trace amount of **14a-Ni$_2$Zn**. Instead, only zinc octaethylporphyrin was obtained in moderate yields.

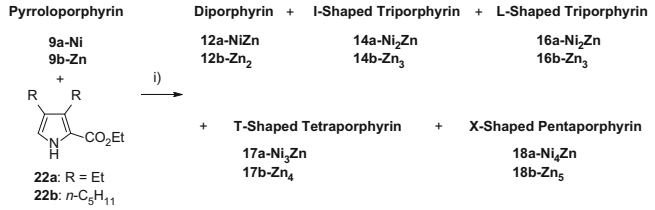

Scheme 2.4 Reagents and conditions: (i) $LiAlH_4$, THF, 0 °C; $BF_3 \cdot OEt_2$, CH_2Cl_2, rt; chloranil, $Zn(OAc)_2 \cdot 2H_2O$, 50 °C

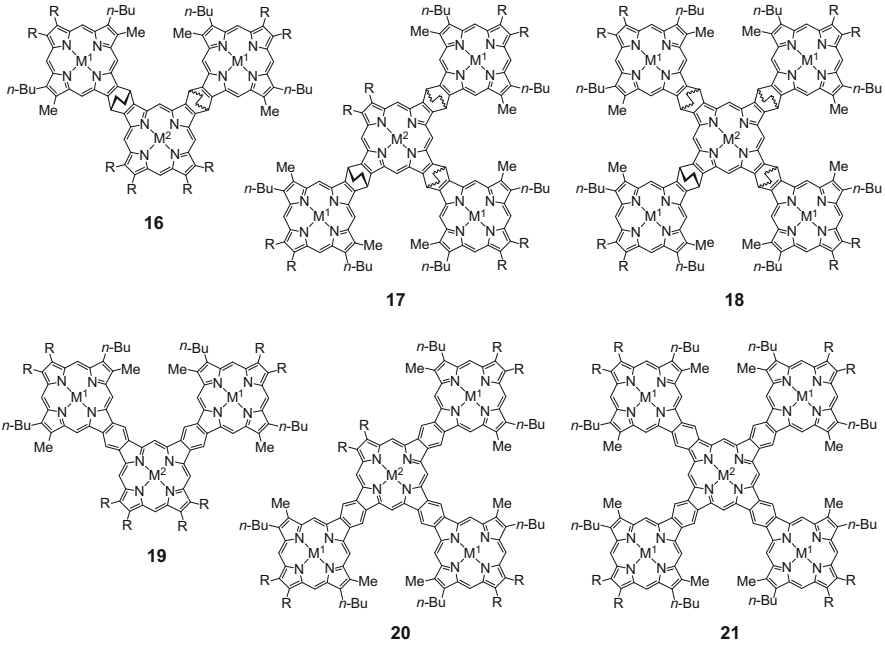

Fig. 2.2 Prepared oligoporphyrins; **a-Ni$_n$Zn**: $M^1 = Ni$, $M^2 = Zn$, R = Et; **a-Zn$_n$**: $M^1 = M^2 = Zn$, R = Et; **b-Zn$_n$**: $M^1 = M^2 = Zn$, R = n-C_5H_{11}

Oligoporphyrins were prepared by the random combination of (hydroxymethyl)pyrroloporphyrins **10** with 3,4-diethyl-2-(hydroxymethyl)pyrrole and 3,4-dipentyl-2-(hydroxymethyl)pyrrole (Scheme 2.4 and Fig. 2.2). An equal molar mixture of **9a-Ni** and ethyl 3,4-diethylpyrrole-2-carboxylate (**22a**) was reduced with $LiAlH_4$ to give a 1:1 mixture of **10a-Ni** and 3,4-diethyl-2-(hydroxymethyl)pyrrole. The mixture was treated with $BF_3 \cdot OEt_2$, oxidized with chloranil, and then reacted with zinc acetate to give a mixture of oligoporphyrins as well as octaethylporphyrin. Diporphyrin **12aa-NiZn** (14 %), I-shaped triporphyrin **14a-Ni$_2$Zn** (10 %), L-shaped triporphyrin **16a-Ni$_2$Zn** (7 %), T-shaped tetraporphyrin **17a-Ni$_3$Zn** (12 %), and X-shaped pentaporphyrin **18a-Ni$_4$Zn** (1 %) were separated by column chromatography followed by preparative GPC. Isomers (C_s and C_2 point groups) of the L-shaped triporphyrin **16a-Ni$_2$Zn** were separated by a combination of

recrystallization and recycled GPC, and the structures were determined by X-ray crystallography. A similar reaction sequence starting from **9b-Zn** and ethyl 3,4-dipenylpyrrole-2-carboxylate (**22b**) provided diporphyrin **12b-Zn$_2$**, I-shaped triporphyrin **14b-Zn$_3$**, L-shaped triporphyrin **16b-Zn$_3$**, T-shaped tetraporphyrin **17b-Zn$_4$**, and X-shaped pentaporphyrin **18b-Zn$_5$**. The pentaporphyrins **18a-Ni$_4$Zn** and **18b-Zn$_5$** were more efficiently prepared by the cyclic tetramerization of **10a-Ni** and **10b-Zn** under conditions similar to random cyclization, with yields of 24 % and 16 %, respectively [24]. All of the zinc oligoporphyrins were quantitatively converted to the corresponding benzene-fused oligoporphyrins **13b-Zn$_2$**, **15b-Zn$_3$**, **19b-Zn$_3$**, **20b-Zn$_4$**, and **21b-Zn$_5$** by heating at 170–200 °C for 30 min in vacuo. TG analysis of **15b-Zn$_3$**, **19b-Zn$_3$**, **20b-Zn$_4$**, and **21b-Zn$_5$** showed single steep weight losses from 150 to 190 °C, corresponding to the expected weights of expelled ethylene molecules.

In the absorption spectra of the benzene-fused tri-, tetra-, and pentaporphyrins, three bands similar to those of the benzene-fused diporphyrins are observed (Table 2.1). As the number of porphyrin rings increased, the absorption maxima of the lowest energy transitions and the intensities also increased. In the X-shaped pentaporphyrin **21b-Zn$_5$**, very strong absorption was observed at 761 (log $\varepsilon = 5.80$) nm in the NIR region. In the case of the L-shaped triporphyrin **19b-Zn$_3$**, sprit Q-band absorptions were observed at 663 and 674 nm with similar intensities of log $\varepsilon = 5.39$ and 5.45, respectively. A single strong Q-band absorption was observed at 680 nm with log $\varepsilon = 5.55$ for the I-shaped triporphyrin **15b-Zn$_3$**. The most striking feature of the L- and I-shaped triporphyrins is the two-photon absorption ability. The two-photon absorbing cross-section value for the I-shaped triporphyrin **15b-Zn$_3$** (2200 GM) is about four times larger than that of the L-shaped triporphyrin **19b-Zn$_3$** (580 GM), which is similar to that of the diporphyrin **12aa-Zn$_2$** (520 GM) [23].

2.3 Diporphyrin Fused with Polycyclic Aromatic Hydrocarbons

Diporphyrins fused with polycyclic aromatic hydrocarbons were then targeted. Scheme 2.5 shows the preparation of naphthalene-fused diporphyrin **27**. The Diels-Alder reaction of triene **22** with tosylacetylene gave a tricyclic vinyl sulfone, which was then subjected to the modified Barton-Zard reaction. Dihydroethanonaphthalene-fused pyrrole **23** was obtained with a good yield [25]. Pyrrole ring construction was achieved at the double bond of **23** by addition of PhSCl, oxidation with mCPBA, dehydrochlorination with DBU, and the Barton-Zard reaction with ethyl isocyanoacetate. Dipyrrole **24** was obtained with a good overall yield. The ester groups of **24** were then removed by thermal treatment in alkaline ethylene glycol to produce α-free dipyrrole **25**. The double [3 + 1] porphyrin synthesis of **25** with tripyrranedicarbaldehyde **8a** gave BCOD-fused porphyrin-benzoporphyrin dyad **26**. Dyad **26** was finally converted to naphthalene-

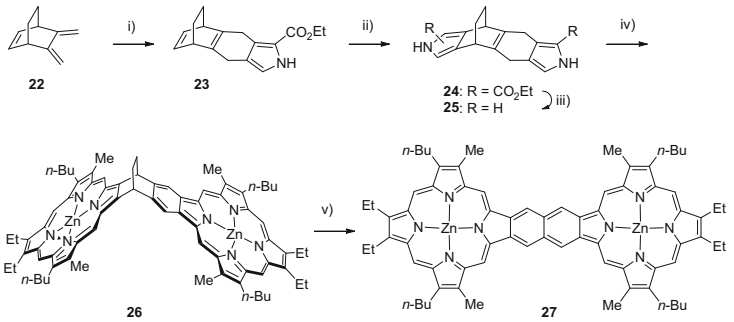

Scheme 2.5 Reagents and conditions: (i) tosylacetylene, $CHCl_3$; $CNCH_2CO_2Et$, KO^{t}Bu, THF, 0 °C; (ii) PhSCl, CH_2Cl_2, 0 °C; *m*CPBA, CH_2Cl_2, rt; $CNCH_2CO_2Et$, KO^{t}Bu, THF, 0 °C; (iii) KOH, ethylene glycol, 170–190 °C; (iv) **8a**, TFA, CH_2Cl_2; DDQ, CH_2Cl_2; Et_3N, $Zn(OAc)_2 \cdot 2H_2O$; (v) 270 °C, in vacuo

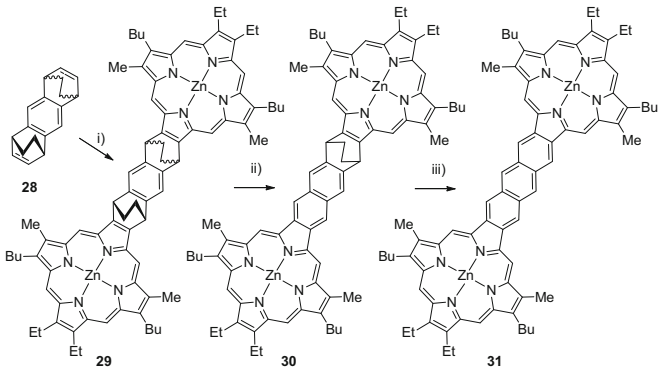

Scheme 2.6 Reagents and conditions: (i) PhSCl, CH_2Cl_2, 0 °C; *m*CPBA, CH_2Cl_2, rt; $CNCH_2CO_2Et$, KO^{t}Bu, THF, 0 °C; KOH, ethylene glycol, 170–190 °C; **8a**, TFA, CH_2Cl_2; DDQ, CH_2Cl_2; Et_3N, $Zn(OAc)_2 \cdot 2H_2O$; (ii) 240 °C for *syn*-**29**, 210 °C for *anti*-**29**, in vacuo; (iii) 320 °C, in vacuo

fused diporphyrin **27** by the retro-Diels-Alder reaction (270 °C, 1 h, in vacuo). TG analysis of **26** revealed that extrusion of the ethylene molecule started from 240 °C and ceased around 270 °C. This conversion temperature was higher than that at which the benzene-fused oligoporphyrins were formed 170 °C.

Diporphyrin fused with anthracene was prepared starting from diethanoanthracene **28** (Scheme 2.6). There are two isomers (*syn*-(C_{2v}) and *anti*-(C_{2h})) in diethanoanthracene **28**, which were selectively prepared. Two porphyrin rings were similarly constructed at the edge of the double bonds of *syn*-**28** and *anti*-**28** to give *syn*-**29** and *anti*-**29**, respectively [26]. From the TG experiments, the first extrusion of ethylene from *syn*-**29** and *anti*-**29** to *anti*-**30** started at about 240 °C and 210 °C, respectively. This difference may be ascribed to the packing of their crystal structures [27]. The second extrusion of the ethylene molecule from **30**

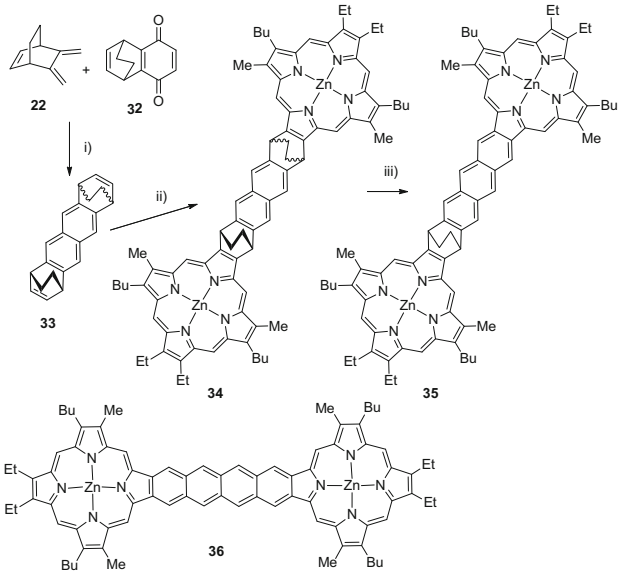

Scheme 2.7 Reagents and conditions: (i) $CHCl_3$, 40 °C, 3 days; $CeCl_3 \cdot 7H_2O$, $NaBH_4$, dioxane/MeOH; 4-M HCl, $CHCl_3$, reflux; DIBALH, CH_2Cl_2, −50 °C; aq-HCl; DDQ, dioxane; (ii) PhSCl, CH_2Cl_2, 0 °C; mCPBA, CH_2Cl_2, 0 °C; DBU, CH_2Cl_2, rt; $CNCH_2CO_2Et$, KO^{t}Bu, THF, rt; KOH, ethylene glycol, 170–190 °C; **8a**, TFA, CH_2Cl_2; DDQ, CH_2Cl_2; Et_3N, $Zn(OAc)_2 \cdot 2H_2O$; (iii) 295 °C, in vacuo, 30 min

occurred at around 310 °C to produce the target anthracene-fused diporphyrin **31**. The intermediate **30** was purified by recrystallization, and the targeted **31** was prepared directly from **29** by heating at 320 °C.

Naphthacene-fused diporphyrins were prepared using Scheme 2.7. The Diels-Alder reaction of triene **22** with ethanonaphthoquinone **32** proceeded smoothly at 40 °C to produce a hexacyclo-endione compound, which was converted to a diastereomeric mixture (1:1) of diethanonaphthacene **33**, by sequential treatment with $NaBH_4$ in the presence of $CeCl_3$, hydrochloric acid, diisobutylaluminium hydride (DIBALH), hydrochloric acid, and 2,3-dichloro-5,6-dicyano-1,4-benzoquinone (DDQ). After the construction of two pyrrole rings at the distal double bonds of **33**, the double [3 + 1] porphyrin synthesis produce the target diethanonaphthacene-fused diporphyrin **34** in moderate yield [26]. The TG experiment of **34** revealed that the extrusion of one ethylene molecule occurred between 250 and 295 °C. The second retro-Diels-Alder reaction, however, occurred from *ca.* 320 °C with concomitant decomposition. No identifiable compounds were obtained, although peaks due to the molecular ions of fully conjugated naphthacene-fused diporphyrin **36** as well as naphthacenoporphyrin were observed in the MALDI-TOF experiment.

Scheme 2.8 shows the synthesis route of diethanopentacene-fused diporphyrin **40**. Triene **22** was reacted with benzadiyne generated by the reaction of

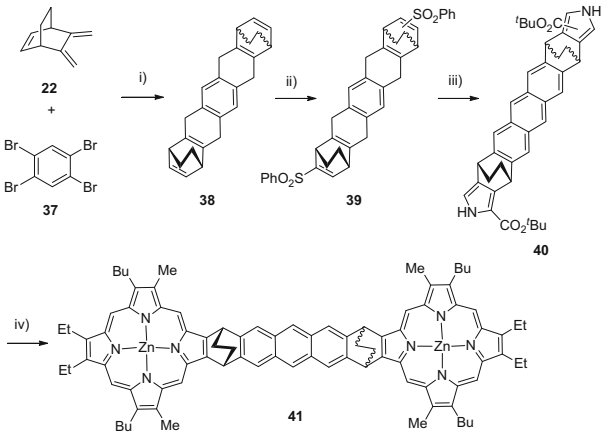

Scheme 2.8 Reagents and conditions: (i) ^{n}BuLi, toluene, 0 °C; (ii) PhSCl, CH_2Cl_2, 0 °C; mCPBA, CH_2Cl_2, 0 °C; DBU, CH_2Cl_2, rt; DDQ, dioxane, rt; $CNCH_2CO_2{}^{t}Bu$, KO^{t}Bu, THF, rt; (iii) TFA, rt, 10 min; **8a**, TFA, CH_2Cl_2, 50 °C; Et_3N, chloranil, CH_2Cl_2; $Zn(OAc)_2 \cdot 2H_2O$

tetrabromobenzene **37** with *n*-butyllithium to give a heptacyclic compound **38**. As the anthracene moiety was also reactive toward a phenylsulfenyl cation, compound **38** was successively treated with phenylsulfenyl chloride, mCPBA, and DBU to give disulfone **39**. Oxidation of **39** with DDQ followed by pyrrole ring construction using *tert*-butyl isocyanoacetate gave dipyrrole **40** as a mixture of four diastereomers. The [3 + 1] porphyrin synthesis of **40** with **8a** gave the target diethanopentacene-fused diporphyrin **41**. The TG experiment of **41** revealed that diporphyrin **41** did not undergo a clean retro-Diels-Alder reaction. Even the first extrusion of the ethylene molecule starting at *ca*. 350 °C was accompanied by decomposition of other parts of the molecule. No identifiable compound was obtained in the thermal treatment of **41**.

Considering that the anthracene fusing unit was the largest linear PAH of the fully conjugated diporphyrins in the preparation based on the retro-Diels-Alder reaction, synthesis of zigzag polycyclic aromatics was targeted next. We planned to prepare chrysene-fused diporphyrin (Scheme 2.9). Diethanochrysene **44** was thought to be the key compound for the preparation of the target chrysene-fused diporphyrin **48**. 1,5-Naphthalenediol (**42**) was reacted with bromine in the presence of iodine to give 2,6-dibromo-1,5-naphthalenediol. After the diol was protected by trimethylsilyl (TMS) groups, bromine-lithium exchange with *n*-butyllithium followed by quenching with TMSCl afforded 2,6-bisTMS-1,5-bisTMSoxynaphthalene, which was converted to bistrifluoromethanesulfonate derivative **43** by deprotection of the TMS ethers followed by quenching the resulting dilithium salt with trifluoromethanesulfonic anhydride. Naphthal-1,5-diyne generated by treatment of **43** with KF with the aid of 18-crown-6 reacted with 1,3-cyclohexadiene to give diethanochrysene **44** in a low yield. In spite of all of our efforts, the yield could not be improved. This low yield was attributed to the intrinsic low reactivity of 1,3-cyclohexadiene,

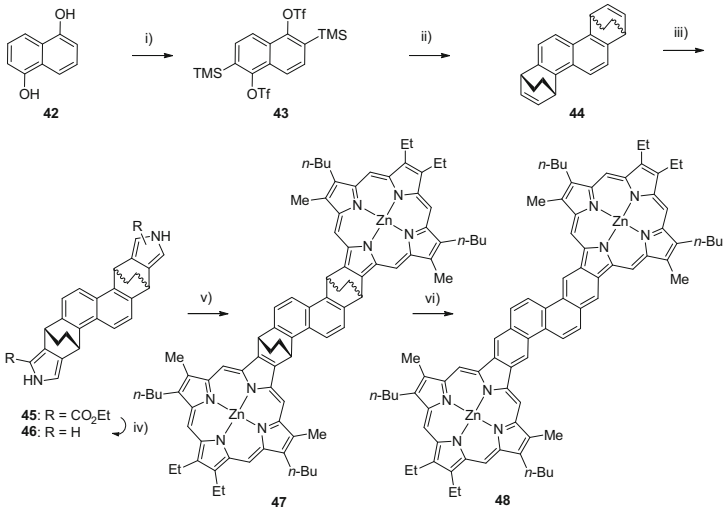

Scheme 2.9 Reagents and conditions: (i) Br_2, I_2 (cat.), AcOH, 80 °C; TMSCl, pyridine, toluene; ^{n}BuLi, TMSCl, THF; ^{n}BuLi, Tf_2O, THF, ether; (ii) 1,3-cyclohexadiene, KF, 18-crown-6; (iii) PhSCl, CH_2Cl_2, 0 °C; mCPBA, CH_2Cl_2, 0 °C; DBU, CH_2Cl_2, rt; DDQ, dioxane, rt; $CNCH_2CO_2Et$, KO^{t}Bu, THF, rt; (iv) KOH, ethylene glycol, 170–190 °C; (v) **8a**, TFA, CH_2Cl_2, 50 °C; Et_3N, DDQ, CH_2Cl_2; $Zn(OAc)_2 \cdot 2H_2O$; (vi) 200 °C, in vacuo

because the naphthaldiyne had smoothly reacted with 1,3-cyclopentadiene to give the corresponding dimethanochrysene in a good yield. The pyrrole ring construction at the distal double bonds of **44** followed by the [3 + 1] porphyrin synthesis afforded diethanochrysene-fused diporphyrin **47** [28]. In the TG experiment with **47**, only one steep weight loss was observed at 180 °C due to two ethylene molecules, and chrysene-fused diporphyrin **48** was obtained.

Electronic spectra of the PAH-fused dizinc diporphyrins are summarized in Table 2.2. In the case of the diethano-PAH-fused dizinc diporphyrins **29**, **34**, **41**, and **47**, no interaction between two zinc-porphyrin chromophores was observed and the absorption spectra were quite similar. This is quite different from the BCOD-fused dizinc porphyrin **12aa-Zn$_2$**, where *homo*-conjugation between the porphyrin chromophores was observed. The Soret- and Q-band absorptions of diethanopentacene-fused dizinc diporphyrin **41** showed a slight bathochromic shift (*ca*. 5 nm), which is probably due to the *homo*-conjugation between the porphyrin and anthracene moieties through the BCOD skeleton. *Homo*-conjugation between porphyrin and acene-fused porphyrin chromophores through the BCOD skeleton was clearly observed in **26**, **30**, and **35**. The absorption maxima of the longer-wavelength Soret absorptions in **26**, **30**, and **35** showed slight bathochromic shift compared to those of benzoporphyrin (416 nm in pyridine) [18], naphthoporphyrin (423 nm in pyridine) [29], and anthroporphyrin (440 nm in pyridine) [30], respectively.

Absorption and TD-DFT calculation (B3-LYP · 6-31 + G(d)/LANL2DZ) spectra of the acene-fused dizinc diporphyrins **13aa-Zn$_2$**, **27**, and **31** are shown in Fig. 2.3

Table 2.2 Absorption and emission maxima of PAH-fused diporphyrins

Diporphyrin	λ_{max}/nm (log ε) Soret band			Q band				Fluorescence
26[a]	414	429			544	582		588
	(5.56)	(5,54)			(4.51)	(4.58)		638
27[a]	414	453	485		584	631		632
	(5.14)	(4.89)	(5.37)		(4.53)	(5.31)		681
29[b]	400				532	570		573
	(5.62)				(4.42)	(4.46)		625
30[c]	414	440		542	575	593	610	591
	(5.54)	(5.60)		(4.42)	(4.49)	(4.56)	(4.51)	638
31[d]	398	484			626	662		665
	1.00[e]	0.88[e]			0.77[e]	0.28[e]		
34[a]	402				532	569		576
	(5.61)				(4.42)	(4.45)		626
35[a]	420	441			607			608
	(5.03)	(4.96)			(4.44)			
41[b]	406				532	571		—[f]
	(5.73)				(4.49)	(4.57)		
47[a]	401				530	568		575
	(5.54)				(4.40)	(4.47)		626
48[c]	429	461			569	604		612
	(5.12)	(5.25)			(4.48)	(4.95)		667

[a]In $CHCl_3$
[b]1% pyridine/$CHCl_3$
[c]In pyridine
[d]In THF
[e]Absorption ratio
[f]Not measured

[31]. In the calculated spectra of the acene-fused dizinc diporphyrins **13aa-Zn$_2$**, **27**, and **31**, the strongest Q-band transitions were at the wavelength close to 595 nm (594–598 nm), while the weaker Q-band transitions showed a bathochromic shift as the acene became higher. In these diporphyrins, the energy levels of the fully delocalized HOMO were higher than those of OMOs, while those of the delocalized LUMO and LUMO + 1 were close. Therefore, these three Frontier orbitals should be considered similar to the cases of phthalocyanines [32]. In the case of **13aa-Zn$_2$**, the LUMO and LUMO + 1 were degenerated so that the calculated Q-band absorptions were similar to those of phthalocyanines: the allowed strong transition from HOMO to LUMO + 1 and the forbidden weak transition from HOMO to LUMO had similar energies. As the fusing units became larger, the energy levels of HOMO and LUMO + 1 increased, while the energy levels of LUMO decreased. Therefore, the strong Q-band absorptions were at similar wavelengths, while the weak Q-band absorptions were at shorter wavelengths in **13aa-Zn$_2$**, at similar wavelengths in **27**, and at longer wavelengths in **31**.

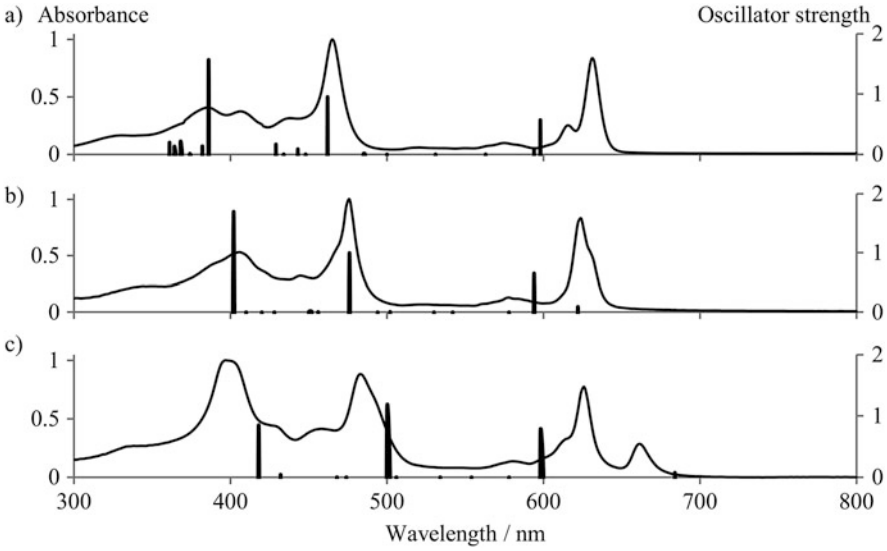

Fig. 2.3 Absorption (1 % pyridine/$CHCl_3$) and TD-DFT calculation (B3-LYP · 6-31 + G(d)/LANL2DZ) spectra of **13aa-Zn$_2$** (**a**), **27** (**b**), and **31** (**c**)

2.4 Conclusion

Oligoporphyrins fused with benzene units and dizinc diporphyrins fused with PAHs were prepared and their electronic properties were examined. The electronic spectra showed strong absorption in the red to NIR region. In the UV-vis spectra of the oligoporphyrins fused with benzene units, three major absorption bands were observed corresponding to two Soret bands and a Q band. A linearly fused trizinc triporphyrin with two benzene moieties showed a strong Q-band absorption, while split Q-band absorptions were observed in an L-shaped triporphyrin. The two-photon absorbing cross-section value for the I-shaped triporphyrin was about four times larger than that for the L-shaped triporphyrin, which was similar to that for diporphyrin. Naphthalene-, anthracene-, and chrysene-fused diporphyrins were successfully prepared, although preparation based on the retro-Diels-Alder reaction of the precursors failed to give naphthacene- and pentacene-fused diporphyrins. The absorption spectra of the benzene-, naphthalene-, and anthracene-fused diporphyrins were well rationalized by the TD-DFT calculations.

2.5 Experiments

Melting points are uncorrected. Unless otherwise specified, NMR spectra were obtained with a JEOL JNM AL-400 spectrometer at room temperature by using $CDCl_3$ as a solvent and tetramethylsilane as an internal standard for 1H and 13C.

FAB and MALDI-TOF mass spectra were measured with an MStation spectrometer (JEOL MS-700) and Voyager DE Pro (Applied Biosystems), respectively. UV-vis and fluorescence spectra were measured on JASCO V-570 and HITACHI F-4500, respectively. Absolute quantum yields were measured on a Hamamatsu Photonics C9920-02. TG analysis was done with SII Exstar 600 TG/DTA 6200. Elemental analysis was performed on a Yanaco MT-5 elemental analyzer. Preparative GPC was performed on JAI-8201 with combination of JAI-gel 1H and 2H columns.

2.5.1 I-Shaped BCOD-Fused Triporphyrin 14a-Ni_2Zn

Red crystals, mp >170 °C (decomp.); *syn*-isomer (C_{2v} isomer): ^{1}H NMR (400 MHz, $CDCl_3$): $\delta = 1.11$ (12H, m), 1.25 (8H, m), 1.72 (8H, m), 1.83 (12H, t, $J = 7.4$ Hz), 2.22 (12H, t, $J = 7.4$ Hz), 2.80 (8H, m), 3.77 (12H, s), 3.95 (16H, m), 4.46 (8H, m), 7.70 (4H, br-s), 9.82 (4H, s), 10.48 (4H, s), 10.82 (4H, s); MALDI-TOF: $m/z = 1657$ ($M^+ - 2C_2H_4$); UV-vis ($CHCl_3$): $\lambda_{max} = 391$, 414, 518, 554, 572 nm; CCDC No 102255 and 1022554.

2.5.2 L-Shaped BCOD-Fused Triporphyrin 16-Ni_2Zn

Red crystals, mp >170 °C (decomp.); *syn*-isomer (C_s isomer): ^{1}H NMR (400 MHz, $CDCl_3$): $\delta = 1.08$ (6H, t, $J = 7.4$ Hz), 1.14 (6H, t, $J = 7.4$ Hz), 1.72 (6H, m), 1.79 (18H, m), 1.99 (6H, m), 2.15 (12H, m), 2.29 (4H, m), 2.80–2.94 (8H, m), 3.76 (6H, s), 3.93 (12H, s), 4.01 (6H, s), 4.07 (4H, m), 4.20 (4H, m), 4.40 (4H, m), 7.74 (2H, br-s), 8.05 (2H, br-s), 9.80 (2H, s), 9.84 (2H, s), 10.27 (1H, s), 10.51 (2H, s), 10.70 (2H, s), 10.82 (2H, s), 11.47 (1H, s); MALDI-TOF: $m/z = 1657$ ($M^+ - 2C_2H_4$); UV-vis ($CHCl_3$): $\lambda_{max} = 394$, 411, 554 nm; CCDC No 1022529.

2.5.3 T-Shaped BCOD-Fused Tetraporphyrin 17-Ni_3Zn

Red crystals, mp >170 °C (decomp.); one isomer: ^{1}H NMR (400 MHz, $CDCl_3$): $\delta = 1.06$–2.97 (66H, m), 3.76 (6H, s), 3.95 (12H, s), 4.00 (16H, m), 4.46 (12H, m), 7.75 (2H, br-s), 9.89 (2H, br-s), 10.49 (2H, s), 10.68 (2H, s), 10.76 (2H, s), 10.87 (2H, s), 11.41 (2H, s); MALDI-TOF: $m/z = 2187$ ($M^+ - 3C_2H_4$); UV-vis ($CHCl_3$): $\lambda_{max} = 394$, 415, 555 nm. Anal. Calcd for $C_{104}H_{112}N_{12}Ni_3Zn \cdot C_6H_{14}$: C, 73.47; H, 6.89; N, 9.45. Found: C, 73.56; H, 7.39; N, 9.19 %.

2.5.4 Diporphyrin Fused with Ethanonaphthalene 26

To a solution of tripyrrane **8a** (109 mg, 0.22 mmol) and dipyrrole **25** (27 mg, 0.11 mmol) in $CHCl_3$ (30 mL) was added trifluoroacetic acid (0.8 mL) under an argon atmosphere. After being stirred for 3 h, the reaction mixture was quenched with triethylamine (1.4 mL) at 0 °C. DDQ (130 mg, 0.57 mmol) was added and the mixture was stirred at room temperature for 5 h. The reaction was quenched with aqueous sat. $NaHCO_3$ and the mixture was extracted with $CHCl_3$. The organic extract was washed with aqueous sat. $NaHCO_3$, water, and brine, dried over Na_2SO_4, and concentrated in vacuo. The residue and $Zn(OAc)_2 \cdot 2H_2O$ (500 mg, 2.27 mmol) were dissolved in a mixture of $CHCl_3$ (50 mL) and MeOH (5 mL), and the mixture was stirred at room temperature for 6 h. The reaction mixture was washed with aqueous sat. $NaHCO_3$, water, and brine, dried over Na_2SO_4, and concentrated in vacuo. The residue was chromatographed on silica gel ($CHCl_3$). The red fractions were collected to leave a red solid after removal of the solvent. Recrystallization of the residue from $CHCl_3$/MeOH gave 34 mg (0.027 mmol, 25 %) of the title compound as dark red crystals: mp > 250 °C (decomp.); ^{1}H NMR (400 MHz, pyridine-d_5): $\delta = 1.12$–1.19 (12H, m), 1.80–1.89 (8H, m), 1.98–2.06 (12H, m), 2.38–2.52 (8H, m), 2.57–2.64 (2H, m), 2.78–2.85 (2H, m), 3.92 (6H, s), 4.02 (6H, s), 4.15–4.40 (16H, m), 7.08 (2H, s), 10.08 (2H, s), 10.59 (2H, s), 10.99 (2H, s), 11.21 (2H, s); UV-vis ($CHCl_3$): λ_{max} (log ε) = 341 (4.69), 414 (5.56), 429 (5.54), 544 (4.51), 582 (4.58) nm; MALDI-TOF: *m/z* = 1238 ($M^+ + 1$); CCDC No 1022865.

2.5.5 Diporphyrin Fused with Naphthalene 27

Ethanonaphthalene-fused diporphryrin **26** was placed in a micro-sample tube, and the tube was placed in a cylinder, which was evacuated by an oil rotary pump. The cylinder was placed in a preheated glass-tube oven (270 °C) for 1 h. The cylinder was cooled to room temperature, and the title compound was taken out from the sample tube: green powder, mp >350 (decomp.); ^{1}H NMR (400 MHz, THF-d_8): $\delta = 1.17$ (12H, t, $J = 7.4$ Hz), 1.80–1.89 (8H, m), 1.94 (12H, t, $J = 7.7$ Hz), 2.38–2.52 (8H, m), 3.84 (12H, s), 4.01–4.22 (16H, m), 10.09 (4H, s), 10.74 (4H, s), 10.79 (4H, s); UV-vis ($CHCl_3$): λ_{max} (log ε) = 349 (4.79), 414 (5.14), 453 (4.89), 485 (5.37), 584 (4.53), 631 (5.31) nm; MALDI-TOF *m/z* 1209 ($M^+ + 1$).

2.5.6 Diporphyrin Fused with Ethanoanthracene 30

syn-Diethanoanthracene-fused diporphryrin **29** was placed in a micro-sample tube, and the tube was placed in a cylinder, which was evacuated by an oil rotary pump. The cylinder was placed in a preheated glass-tube oven (320 °C) for 1 h. The cylinder was cooled to room temperature, and the title compound was taken out from

the sample tube: dark purple powder, mp > 350 °C (decomp.); ^{1}H NMR (400 MHz, pyridine-d_5): $\delta = 1.07$–1.14 (12H, m), 1.71–1.84 (8H, m), 1.91–1.99 (12H, m), 2.31–2.46 (10H, m), 2.60–2.67 (2H, m), 3.69 (6H, s), 3.85 (6H, s), 40.9–4.31 (16H, m), 6.75 (2H, s), 9.04 (2H, s), 10.43 (2H, s), 10.46 (2H, s), 10.52 (2H, s), 10.92 (2H, s), 10.98 (2H, s); UV-vis (pyridine): λ_{max} (log ε) = 341 (4.75), 414 (5.54), 440 (5.60), 542 (4.42), 575 (4.49), 593 (4.56), 610 nm (4.51); MALDI-TOF: *m/z* = 1259 ($M^+ + 1$); CCDC No 1024855.

2.5.7 Diporphyrin Fused with Anthracene 31

syn-Diethanoanthracene-fused diporphryrin **29** was placed in a micro-sample tube, and the tube was placed in a cylinder, which was evacuated by an oil rotary pump. The cylinder was placed in a preheated glass-tube oven (240 °C) for 1 h. The cylinder was cooled to room temperature, and the title compound was taken out from the sample tube: dark purple powder, mp >320 °C (decomp.); ^{1}H NMR (400 MHz, THF-d_8): $\delta = 1.03$ (12H, m), 1.82 (12H, m), 2.20–2.40 (8H, m), 2.80–3.40 (8H, m), 3.80–4.20 (16H, m), 4.59 (12H, s), 8.81 (2H, s), 9.94 (4H, s), 10.05 (4H, s), 10.42 (4H, s); UV-vis (pyridine): $\lambda_{max} = 398$, 484, 626, 662 nm; MALDI-TOF: *m/z* = 1288 ($M^+ + 1$). Anal. Calcd for $C_{80}H_{86}N_8Zn_2$: C, 74.46; H, 6.72; N, 8.68. Found: C, 74.15; H, 7.04; N, 8.82 %.

2.5.8 Diporphyrin Fused with Ethanonaphthacene 35

Diethanonaphthacene-fused diporphyrin **34** [28] (2.60 mg) was placed in a micro-sample tube, and the tube was placed in a cylinder, which was evacuated by an oil rotary pump. The cylinder was placed in a preheated glass-tube oven (295 °C) for 1 h. The cylinder was cooled to room temperature, and the title compound was taken out from the sample tube: green powder, mp >350 (decomp.); ^{1}H NMR (400 MHz, pyridine-d_5): $\delta = 1.02$–1.17 (12H, m), 1.25–1.32 (4H, m), 1.75–1.84 (8H, m), 1.92–1.98 (12H, m), 2.33–2.43 (8H, m), 3.64 (6H, s), 3.80 (6H, s), 4.13–4.20 (16H, m), 9.37 (2H, br-s), 9.86 (2H, s), 9.95 (2H, s), 10.38 (2H, s), 10.45 (2H, s), 10.52 (2H, s), 10.82 (2H, m), 10.99 (2H, s); MALDI-TOF: *m/z* = 1341 ($M^+ + 5$), 1313 ($M^+ + 5 - C_2H_4$); UV-vis ($CHCl_3$): λ_{max} (log ε) = 420 (5.03), 441 (4.96), 6.7 (4.44).

2.5.9 Diporphyrin Fused with Diethanopentacene 41

Trifluoroacetic acid (0.51 mL, 6.48 mmol) was added to dipyrrole **40** (73.6 mg, 0.12 mmol) at 0 °C, and the solution was stirred at room temperature for 10 min. Tripyrrane **8a** (114.6 mg, 0.24 mmol) in dry CH_2Cl_2 (15 mL) was added, and the

reaction mixture was stirred at 50 °C for 1 h under nitrogen in the dark. After being neutralized with triethylamine (0.80 mL, 5.76 mmol) at 0 °C, the reaction mixture was oxidized with chloranil (59.0 mg, 0.24 mmol) at room temperature for 1 h. The reaction mixture was quenched with an aqueous solution of $Na_2S_2O_3$ and extracted with CH_2Cl_2. The organic layer was washed successively with water, an aqueous solution of $NaHCO_3$, and brine, then dried over Na_2SO_4, and concentrated. The residue was dissolved in $CHCl_3$ (15 mL) and $Zn(OAc)_2.2H_2O$ (52.7 mg, 0.24 mmol) was added. The mixture was stirred at room temperature overnight under N_2. Following that, the reaction mixture was washed with water and an aqueous solution of $NaHCO_3$, dried over Na_2SO_4, and concentrated. The residue was chromatographed on silica gel ($CHCl_3$, Rf = 0.88) and recrystallized from THF/MeOH to afford **41** as a purple powder (22.7 mg, 13 %): mp 257 °C (decomp.); UV-vis ($CHCl_3$): λ_{max} (log ε) 406 (5.73), 532 (4.49), 571 (4.57); ^{1}H NMR (400 MHz, THF-d_8): $\delta = 1.08$ (12H, t $J = 7.8$ Hz), 1.74 (8H, m), 1.89 (12H, t $J = 8.1$ Hz), 2.18 (4H, m), 2.28 (8H, m), 2.34 (4H, m), 3.70 (12H, s), 4.12 (16H, m), 6.18 (4H, s), 8.19 (4H, s), 8.36 (2H, s), 10.09 (4H, s), 10.33 (4H, s); ^{13}C NMR (100 MHz, THF-d_8): $\delta = 11.09$, 11.15, 13.75, 13.83, 18.31, 18.39, 19.64, 19.72, 22.94, 23.02, 26.13, 26.19, 29.80, 35.66, 35.73, 40.31, 78.54, 96.29, 96.40, 97.48, 97.56, 107.00, 120.71, 125.00, 130.98, 135.90, 140.73, 140.83, 141.74, 141.84, 142.08, 142.18, 143.22, 143.24, 147.43, 147.47, 148.10, 148.24; IR (KBr): $\nu_{max} = 2952$, 2929, 2860, 771 cm^{-1}; MALDI-TOF: *m/z* =1418 (M^+ +4), 1392, 1362; HRMS (FAB$^+$) Calcd for $C_{90}H_{94}N_8Zn_2 + H^+$: 1415.6263. Found: 1415.6262. Anal. Calcd for $C_{90}H_{94}N_8Zn_2 + C_4H_8O$: C, 75.74; H, 6.90; N, 7.52. Found: C, 75.74; H, 6.89; N, 7.33 %.

2.5.10 Diporphyrin Fused with Chrysene 48

Diethanochrysene-fused diporphyrin **47** [28] (3.0 mg) was placed in a micro-sample tube, and the tube was placed in a cylinder, which was evacuated by an oil rotary pump. The cylinder was placed in a preheated glass-tube oven (250 °C) for 2 h. The cylinder was cooled to room temperature and the title compound was taken out from the sample tube: green powder, mp >350 (decomp.); ^{1}H NMR (400 MHz, pyridine-d_5): $\delta = 1.13$ (12H, t, $J = 7.4$ Hz), 1.96–2.00 (20H, m), 2.42(8H, q, $J = 7.1$ Hz), 3.84 (6H, s), 3.85 (6H, s), 4.07–4.32 (16H, m), 9.02 (2H, d, $J = 9.2$ Hz), 10.03 (2H, d, $J = 9.2$ Hz), 10.51 (4H, s), 10.54 (2H, s), 11.08 (2H, s), 11.40 (2H, s), 11.72 (2H, s); IR (KBr) $\nu_{max} = 2954$, 2925, 2859, 1538, 1010 cm^{-1}; UV-vis (pyridine): λ_{max} (log ε) = 429 (5.12), 461 (5.25), 569 (4.48), 604 (4.95) nm; MALDI-TOF: *m/z* = 1313.02 (M^+ +5); CCDC No 1023537.

References

1. Cui S, Yin D, Chen Y, Di Y, Chen H, Ma Y, Achilefu S, Gu Y (2013) ACS Nano 22:676–688; Xia L, Kong X, Liu X, Tu L, Zhang Y, Chang Y, Liu K, Shen D, Zhao H, Zhang H (2014) Biomaterials 35:4146–4156
2. Jechow A, Seefeldt M, Kurzke H, Heuer A, Menzel R (2013) Nat Photonics 7:973–976; Yang P, Shi L, Pratavieira S, Alfano RR (2013) J Appl Phys 114:153102
3. Hamamura T, Nakazaki J, Uchida S, Kubo T, Segawa H (2014) Chem Lett 43:655–657; Kinoshita T, Dy JT, Uchida S, Kubo T, Segawa H (2013) Nat Photonics 7:535–539
4. Fabian J, Nakazumi H, Matsuoka M (1992) Chem Rev 92:1197–1226
5. Anderson RR, Parrish JA (1981) J Investig Dermatol 77:13–19
6. Shalav A, Richards BS, Trupke T, Krämer KW, Güdel HU (2005) Appl Phys Lett 86:013505
7. Wicklein A, Lang A, Muth M, Thelakkat M (2009) J Am Chem Soc 131:14442–14453
8. Nakamura M, Tahara H, Takahashi K, Nagata T, Uoyama H, Kuzuhara D, Mori S, Okujima T, Yamada H, Uno H (2012) Org Biomol Chem 10:6840–6849
9. Yamamoto A, Ohta E, Kishigami N, Tsukahara N, Tomiyori Y, Sato H, Matsui Y, Kano Y, Mizuno K, Ikeda H (2013) Tetrahedron Lett 54:4049–4053; Wasserfallen D, Kastler M, Pisula W, Hofer WA, Fogel Y, Wang Z, Müllen K (2006) J Am Chem Soc 128:1334–1339
10. Oyaizu K, Iwasaki T, Tsukahara Y, Tsuchida E (2004) Macromolecules 37:1257–1270; Shinamura S, Osaka I, Miyazaki E, Takimiya K (2011) Heterocycles 83:1187–1204
11. Yamaguchi S, Xu C, Yamada H, Wakamiya A (2005) J Org Chem 690:5365–5377; Matano Y, Saito A, Fukushima T, Tokudome Y, Suzuki F, Sakamaki D, Kaji H, Ito A, Tanaka K, Imahori H (2011) Angew Chem Int Ed 50:8016–8020; London G, von Wantoch Rekowski M, Dumele O, Schweizer WB, Gisselbrecht J-PL, Boudon C, Diederich F (2014) Chem Sci 5:965–972; Wang X-Y, Zhuang F-D, Wang R-B, Wang X-C, Cao X-Y, Wang J-Y, Pei J (2014) J Am Chem Soc 136:3764–3767; Levine DR, Siegler MA, Tovar JD (2014) J Am Chem Soc 136:7132–7139; Kato S, Furuya T, Kobayashi A, Nitani M, Ie Y, Aso Y, Yoshihara T, Tobita S, Nakamura Y (2012) J Org Chem 77:7595–7606
12. Nakamura M, Kitatsuka M, Takahashi K, Nagata T, Mori S, Kuzuhara D, Okujima T, Yamada H, Nakae T, Uno H (2014) Org Biomol Chem 12:1309–1317; Yamada H, Okujima T, Ono N (2008) Chem Commun 2957–2974
13. Takase M, Enkelmann V, Sebastiani D, Baumgarten M, Müllen K (2007) Angew Chem Int Ed 46:5524–5527
14. Müllen K, Rabe JP (2008) Acc Chem Res 41:511–520
15. Ghoroghchian PP, Frail PR, Susumu K, Blessington D, Brannan AK, Bates FS, Chance B, Hammer DA, Therien MJ (2004) Proc Natl Acad Sci U S A 102:2922–2927
16. Balaz M, Collins HA, Dahlstedt E, Anderson HL (2009) Org Biomol Chem 7:874–888
17. Kim KS, Lim JM, Osuka A, Kim D (2008) J Photochem Photobiol C 9:13–28
18. Uoyama H, Takiue T, Tominaga K, Ono N, Uno H (2009) J Porphyrins Phthalocyanines 13:122–135
19. Uno H, Hashimoto M, Fujimoto A (2009) Heterocycles 77:887–898
20. Ito S, Nakamoto K, Uno H, Murashima T, Ono N (2001) Chem Commun 2696–2697; Ono N, Kuroki K, Watanabe E, Ochi N, Uno H (2004) Heterocycles 62:365–373
21. Uno H, Nakamoto K, Kuroki K, Fujimoto A, Ono N (2007) Chem Eur J 13:5773–5784
22. Bhattacharya S, Hashimoto M, Fujimoto A, Kimura T, Uno H, Komatsu N (2008) Spectrochim Acta A 70A:416–424
23. Kim P, Ham S, Oh J, Uoyama H, Watanabe H, Tagawa K, Uno H, Kim D (2013) Phys Chem Chem Phys 15:10612–10615
24. Uoyama H, Kim KS, Kuroki K, Shin J-Y, Nagata T, Okujima T, Yamada H, Ono N, Kim D, Uno H (2010) Chem Eur J 16:4063–4074
25. Okujima T, Jin G, Hashimoto Y, Yamada H, Uno H, Ono N (2006) Heterocycles 70:619–626
26. Uno H, Furukawa M, Fujimoto A, Uoyama H, Watanabe H, Okujima T, Yamada H, Mori S, Kuramoto M, Iwamura T, Hatae N, Tani F, Komatsu N (2011) J Porphyrins Phthalocyanines 15:951–963

27. Uno H, Masumoto A, Ono N (2003) J Am Chem Soc 125:12082–12083
28. Mori S, Kawamoto N, Okujima T, Uno H. manuscript in preparation
29. Ito S, Ochi N, Uno H, Murashima T, Ono N (2000) Chem Commun 2000:893–894
30. Cai C, Uoyama H, Nakamura M, Uno H (2012) Heterocycles 84:829–841; Uoyama H, Yamada H, Okujima T, Uno H (2012) Heterocycles 86:515–534
31. Frisch MJ, Trucks GW, Schlegel HB, Scuseria GE, Robb MA, Cheeseman JR, Scalmani G, Barone V, Mennucci B, Petersson GA, Nakatsuji H, Caricato M, Li X, Hratchian HP, Izmaylov AF, Bloino J, Zheng G, Sonnenberg JL, Hada M, Ehara M, Toyota K, Fukuda R, Hasegawa J, Ishida M, Nakajima T, Honda Y, Kitao O, Nakai H, Vreven T, Montgomery JA, Peralta JE Jr, Ogliaro F, Bearpark M, Heyd JJ, Brothers E, Kudin KN, Staroverov VN, Keith T, Kobayashi R, Normand J, Raghavachari K, Rendell A, Burant JC, Iyengar SS, Tomasi J, Cossi M, Rega N, Millam JM, Klene M, Knox JE, Cross JB, Bakken V, Adamo C, Jaramillo J, Gomperts R, Stratmann RE, Yazyev O, Austin AJ, Cammi R, Pomelli C, Ochterski JW, Martin RL, Morokuma K, Zakrzewski VG, Voth GA, Salvador P, Dannenberg JJ, Dapprich S, Daniels AD, Farkas O, Foresman JB, Ortiz JV, Cioslowski J, Fox DJ (2010) Gaussian 09, Revision C.01; Gaussian, Inc., Wallingford
32. Ishii K, Kobayashi N (2000) The photophysical properties of phthalocyanines and related compounds. In:Kadish KM, Smith KM, Guilard G (eds) The porphyrin handbook, vol 16. Academic Press, San Diego, pp 1–40

http://www.springer.com/978-4-431-55356-4

Chemical Science of π-Electron Systems

Akasaka, T.; Osuka, A.; Fukuzumi, S.; Kandori, H.; Aso, Y. (Eds.)

2015, XVI, 777 p. 583 illus., 215 illus. in color.,
Hardcover
ISBN: 978-4-431-55356-4